



Broom Fibers as Reinforcing Materials for Polypropylene-Based Composites

Ramiro Dell'Erba, Maurizio Avella, Luca Casale, Bonaventura Focher, Ezio Martuscelli, Annamaria Marzetti

► To cite this version:

Ramiro Dell'Erba, Maurizio Avella, Luca Casale, Bonaventura Focher, Ezio Martuscelli, et al.. Broom Fibers as Reinforcing Materials for Polypropylene-Based Composites. *Journal of Applied Polymer Science*, 1998, 68 (7), pp.1077-1089. 10.1002/(SICI)1097-4628(19980516)68:73.0.CO;2-C . hal-01998429

HAL Id: hal-01998429

<https://hal.science/hal-01998429>

Submitted on 5 Mar 2019

HAL is a multi-disciplinary open access archive for the deposit and dissemination of scientific research documents, whether they are published or not. The documents may come from teaching and research institutions in France or abroad, or from public or private research centers.

L'archive ouverte pluridisciplinaire **HAL**, est destinée au dépôt et à la diffusion de documents scientifiques de niveau recherche, publiés ou non, émanant des établissements d'enseignement et de recherche français ou étrangers, des laboratoires publics ou privés.



Italian National Agency for New Technologies, Energy and Sustainable Economic Development

<http://www.enea.it/en>

<http://robotica.casaccia.enea.it/index.php?lang=en>

This paper is a pre-print. The final paper is available on:

D7. Journal of Applied Science “ Broom fibers as reinforcing materials for polypropylene based composites” M. Avella, L. Casale, R. dell’Erba, B. Focher, E. Martuscelli and A. Marzetti 68, 1077-1089 (1998).

Broom Fibers as Reinforcing Materials for Polypropylene-Based Composites

MAURIZIO AVELLA,¹ LUCA CASALE,¹ RAMIRO DELL'ERBA,¹ BONAVENTURA FOCHER,² EZIO MARTUSCELLI,¹ ANNAMARIA MARZETTI¹

¹ Istituto di Ricerca e Tecnologia delle Materie Plastiche, C.N.R., Via Toiano 6, 80072 Arco Felice (Napoli), Italy

² Stazione Sperimentale per la Cellulosa, Carta e Fibre Tessili Vegetali ed Artificiali, Piazza Leonardo da Vinci 26, 20133 Milano, Italy

ABSTRACT: Broom fibers have been used as reinforcement for the conventional polypropylene (iPP) and a maleate modified one (iPPMA). A conventional alkaline treatment and a steam explosion extraction process were applied to obtain the cellulosic material from broom branches. Composites were prepared by melt mixing materials with different weight percentages of broom fibers. Also ternary blends (iPPMA/iPP/broom fibers 5/45/50 wt) were obtained to examine the possibility of utilizing the maleate polypropylene as a compatibilizing agent. The fibers and the composites were thermally, morphologically, and mechanically characterized. Water absorption tests, to examine the behavior of these materials in wet conditions, were also performed. Particular attention was addressed to the study of the fiber/matrix interfacial adhesion. The results showed that the iPPMA-based composites, reinforced with alkaline extracted broom fibers, present specific mechanical properties competitive with those of the homologous polypropylene-based materials reinforced with short glass fibers. The ternary blends gave similar properties to those of the corresponding whole iPPMA-based composites. It is considered that the esteric linkage between the cellulose —OH, and the maleic anhydride groups grafted on the polypropylene backbone is greatly responsible for the similarity in the properties. In spite of better adhesion observed in the samples reinforced by the steam-exploded fibers, less improvement of the mechanical properties was observed, owing to significant damage of the structure of the fibers during the steam explosion process. A general decrease of mechanical properties is observed in normal polypropylene-based composites. The results are also supported by the water absorption tests: whereby the iPPMA-based composites showed good capability to return their dry properties when kept in an oven after wetting for many days. © 1998 John Wiley & Sons, Inc. *J Appl Polym Sci* 68: 1077–1089, 1998

Key words: broom fibers; polypropylene-based composites

INTRODUCTION

Vegetable fibers are increasingly finding applications in polymeric reinforcements because of their desirable characteristic such as high specific prop-

erties.^{1,2} They are also biodegradable, renewable, and of low cost. The reinforcement potential of plant fibers lies on their cellulose content, fiber size, and hydrogen surface bonds.^{3,5} Some studies have been reported on composites^{6,7} based on a biodegradable polyhydroxybutyrate (PHB) and polypropylene matrices reinforced by the steam-exploded wheat straw fibers.^{6–8}

The steam explosion technique is a physical

process applied on a wooden structure. It separates the lignocellulosic material into its main components, namely cellulose fibers, amorphous lignin, and hemicellulose. The last two substances are then removed and strong fibers with a high content of cellulose are finally produced. Fibers obtained through this process are known to be more reactive due to increased surface area.⁹

However, the steam explosion process has the disadvantage of producing relatively short fibers. This renders steam-exploded fibers reinforced composites inferior in certain properties compared to those of synthetic fiber-reinforced composites such as glass fiber-reinforced thermosets and thermoplastics.^{6,7}

In this work an attempt has been made to apply the steam explosion technique on broom branches, from bottom plants, known to have a high content of cellulose, good mechanical properties, and also because they are readily available in Italy and in the Mediterranean countries. Moreover, the plants require less care and can be planted annually.

A traditional chemical extraction process that uses an alkaline sodium hydroxide solution has also been applied on the same wooden material. Fibers extracted by the two methods have been used as reinforcement for the two commercial polypropylenes: the conventional isotactic polypropylene, and maleic anhydride (iPPMA).¹⁰ The composites have also been subjected to water absorption treatment.

To assess the reinforcement effect fibers, composite characterization techniques and mechanical properties determination have been performed with particular attention on the fiber–matrix interfacial characteristic. The results have been compared with those of short glass reinforced polypropylene composites.

EXPERIMENTAL

Materials

The broom branches, from which broom fibers have been extracted, were supplied by SIVA-Italy. The isotactic polypropylene (iPP) and the maleate-modified polypropylene (iPPMA) were supplied by Montell Italia. Some of the characteristics of the two polypropylene polymers have been provided in Table I.

Fiber Extraction

The broom branches were subjected to two different fiber extraction processes: the alkaline treatment process, in which broom branches were heated to 40°C for 20 min in an aqueous solution of 4% (wt) sodium hydroxide. The fibers obtained were washed in water and dried, and the steam explosion process whereby broom branches were steam heat at 190°C under steam pressure of about 20 bar for 2 min using a Delta Lab EC 300. The extracted fibers were then dried in an oven at 80°C for enough time to remove water absorbed during the steam explosion process.

Specimen Preparation

The fibers obtained from the two extraction processes were compounded with the polypropylenic matrices by melt mixing, using a Brabender-like apparatus (Rheocord EC, Haake Inc.) operating at 190°C for 10 min. The material obtained was used to prepare 1 and 3 mm thickness sheets, for tensile and impact tests, respectively. Steel frame molds measuring $10 \times 7 \times 0.1$ cm and $6.5 \times 6.5 \times 0.3$ were placed one at a time, between plates of an electrically heated hydraulic press. They were then heated at 190°C, without applying any pressure, for 7 min, to allow complete melting of the matrix, and subsequently for an additional 3 min at a pressure of 10 MPa. The composites were slowly cooled to room temperature and then released from the mold.

Some composites were also prepared using the fibers obtained from the two extraction process and polypropylene, to which a small percentage of iPPMA (5%) had been added, to determine if the modified polypropylene can be used as a compatibilizing agent and impact improvement in the mechanical properties of the resulting composites. All examined samples in Table II are listed and coded.

Techniques

Wide-angle X-ray spectroscopy (WAXS) was used to determine the structure of the fibers obtained by the two extraction procedures. Here, the lignocellulosic material, in provider form, was subjected to a Ni-filtered CuK_α radiation using a Siemens 500 D Diffractometer equipped with a scintillator counter and a linear amplifier.

Morphological studies on the fibers were carried out by scanning electron microscopy (SEM)

Table I Characteristics of Polypropylenes Used

Materials	Density (g/cm ³)	T_m^a (°C)	T_d^b (°C)	Maleic Anhydride Content (% wt)	η_{inh}^c (dL/g)
iPP	0.9	170	282	0	0.97
iPPMA	0.9	160	274	1.6	1.09

^a Melting temperature determined by means of differential scanning calorimetry.

^b Degradation temperature, determined by means of thermogravimetric analysis, at which 10% wt of the sample is degraded.

^c In 1,2,4-trichlorobenzene, 135°C.

using a Philips 501 SEM after metallization of the fiber surfaces by means of a Polaron sputtering apparatus with Au–Pd alloy.

The thermal investigation on the composite materials was performed by means of a differential scanning calorimeter (DSC) Mettler TA-3000 equipped with control and programming unit (microprocessor TC-10), operating under nitrogen atmosphere. The apparent melting temperatures (T'_m), the crystallization temperature (T_c), and the crystallinity indices (X_c), determined by DSC, were measured with a precision of 0.2°C and 5% on the temperature and the X_c values, respectively. The melting temperature observed (T'_m), the crystallization temperature (T_c), and the apparent melting (or crystallization) enthalpy (ΔH^*) of each sample were obtained from the maxima and the area of the melting (or crystallization) peaks, respectively. The crystallinity indices of the samples were calculated by the following relation:

$$X_c = \frac{\Delta H^*}{\Delta H^\circ}$$

where ΔH° is the specific heat of fusion of 100% crystalline iPP, taken as 209 J/g.¹¹

The measurements were performed by using two different thermal cycles. Cycle A—first fusion: from 30 to 200°C, with a scan rate of 20°C/min, followed by an isotherm at 200°C for 10 min; quenching: from 200 to –50°C, with a scan rate of 100°C/min. Second fusion: from –50 to 200°C, with a scan rate of 20°C/min (in this run the glass transition could be observed). Cycle B—first fusion: from 30 to 200°C, with a scan rate of 20°C/min, followed by an isotherm at 200°C for 10 min; crystallization: from 200 to 30°C, with a scan rate of 10°C/min. Second fusion: from 30 to 200°C, with a scan rate of 10°C/min.

The former determined the glass transition temperature (T_g), and the latter was run to obtain the other values (T_m , T_c , and X_c).

Optical microscopy technique was carried out to investigate the nucleating ability of the fibers on the polypropylenic matrices. This was performed by using a Reichert optical microscope operating in polarized light, equipped with a Mettler apparatus for temperature control, working in a temperature range between 30 and 300°C. The measurements were realized by placing an iPPMA film on a broom fiber (NaOH extracted), placed on a microscope slide, on top of which was put a cover slide to hold the specimen on place. The samples obtained were heated at 200°C and kept for 10 min at this temperature. They were then cooled to a prefixed T_c , to provide isothermal crystallization. Micrographs of the growing spherulites were made at this crystallization temperature.

The mechanical behavior of composites was examined by tensile and fracture tests.

Tensile tests were performed according to the ASTM D638 standard (samples of type IV, 1-mm thickness) by using an Instron machine (model 1122) at a crosshead speed of 1 mm/min. From the stress–strain curves, Young tensile modulus (E), tensile strength at break (σ_b), and percent elongation at break (ϵ_b), were determined.

Fracture tests were carried out on a Charpy Instrument Pendulum (Ceast Autographic Pendulum MK2) at an impact speed of 1 m/s (ASTM D256). For this test, the samples (in the form of small bars with dimensions 6.5 × 0.6 × 0.3 cm) were notched as follows: first, a blunt notch was produced by using a machine with a V-shaped tool, and then a sharp notch of ~ 0.2-mm depth was made by a razor blade fixed to a micrometric apparatus. The final value of notch depth was measured after fracture by using an optical microscope. The samples, with a notch depth-to-width ratio of 0.3 and a span test of 48 mm, were fractured at room temperature. The relative curves of energy and load, plotted vs. time, were recorded, and the critical strain energy release (G_c) and the

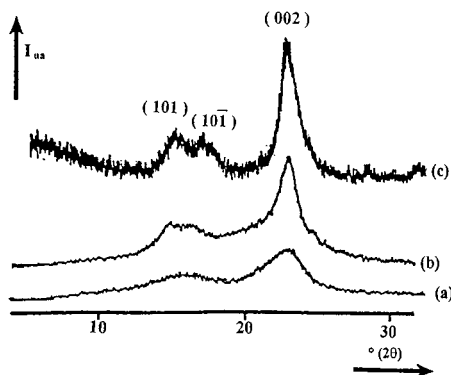


Figure 1 WAXS diffraction patterns: (a) NaOH-extracted fiber, (b) SEP fiber, (c) pure cellulose in the crystallographic form I.

critical stress intensity factor (K_{Ic}) were calculated according to the linear elastic fracture mechanics (LEFM) theory.^{12,13}

The fracture surface of the samples after impact tests were observed by SEM apparatus, after metallization, to investigate the fiber/matrix adhesion for these materials.

The resistance of the fiber/matrix interface to the water penetration in the composites was examined by immersion in aqueous of a 1-mm sheet for 1 month, periodically measuring the increase in weight of the samples (ASTM D570). After saturation, tensile tests were also performed, on the same samples, both on the wet ones and on those dried in an oven at 50°C for 24 h to verify the residual mechanical properties of the materials. Afterwards the amount of water entrapped inside the materials was determined using the thermogravimetric analysis (TGA): wet and dried samples were kept for 30 min at 140°C, measuring the consequent weight reduction.

RESULTS AND DISCUSSION

Fiber Characterization

WAXS Analysis

In Figure 1 the WAXS diffraction patterns for NaOH-extracted broom fibers, SEP broom fibers, and pure cellulose in the crystallographic form I are reported.

From these graphics the following can be observed: (1) Both extracted fibers are in the crystallographic form I of the cellulose. Both spectra show the 22.6° (2θ) reflection related to the (002) crystallographic plane and the two broad and un-

resolved reflections in the range from 13 to 18° (2θ) corresponding to the (10 $\bar{1}$) and the crystallographic planes of cellulose I, respectively. (2) The SEP extracted fibers are characterized by a higher degree of crystallinity with respect to the NaOH-treated ones. The crystallinity indices, calculated according to the Segal method,¹⁴ are $(I_c)_{SEP} = 0.77$ and $(I_c)_{NaOH} = 0.60$, respectively. (3) Finally, the sharpness of all the reflections clearly show that, in the case of SEP extracted fiber, the crystal size seems to be higher with respect to that of NaOH extracted one.

These different crystallization behaviors can be related, in the case of SEP treatment, to a reorganization at high temperatures of amorphous and/or paracrystalline cellulose regions releasing the strains existing in the native cellulose, mainly due to the interactions with hemicelluloses and lignin.⁸

SEM Analysis

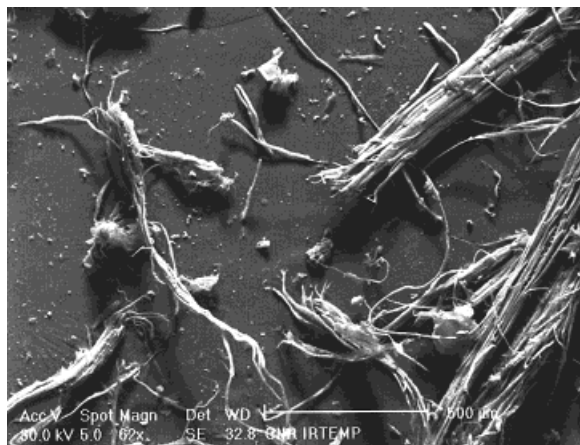
In Figure 2(a,b) and 3(a,b) the SEM micrographs for NaOH-extracted broom fibers and SEP broom fibers are reported, respectively. From these figures it can clearly be deduced that the exploded fibers present a smooth and clean surface with respect to the alkaline-treated ones, confirming that the steam explosion process, performed on lignocellulosic materials, produces an effective strong defibrillation giving rise to a high number of single shorter fibers [see Fig. 3(a)]. Moreover, it seems that the NaOH-extracted fibers are not single separated, but rather bundled.

It should be noted that in addition to the structural modification of wood, as described above, there are also mechanical effects; this last, owing to the adiabatic expansion of vapor, produce morphological variations able to increase the specific surface. This led to a higher reactivity of SEP and resulted in higher availability of the hydroxyl groups distributed on the surface of cellulose.⁶

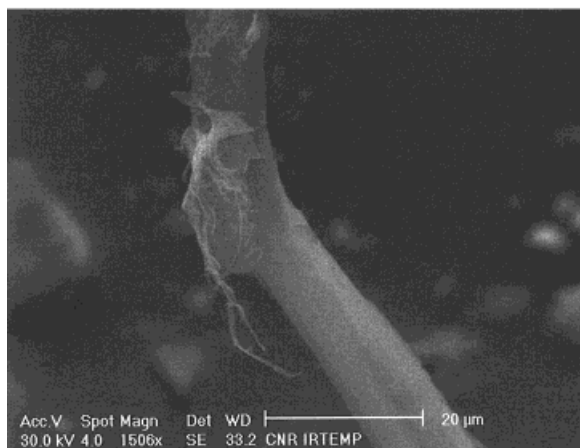
Composites Characterization

Thermal Analysis

In Tables III, IV, and V the findings obtained from DSC measurements, for NaOH-extracted fibers and SEP-extracted fibers, iPPMA-based composites and iPP-based materials, are listed, respectively. The calculated thermal parameters are: the apparent melting temperature measured in the first fusion run ($T_m[I]$) and in the second fusion run ($T_m[II]$), the crystallization tempera-



(a)



(b)

Figure 2 SEM micrographs: NaOH-extracted broom fibers. (a) $\times 40.3$; (b) $\times 686.4$.

ture (T_c), the crystallinity indices for the three processes (X_c), and the glass transition temperature (T_g).

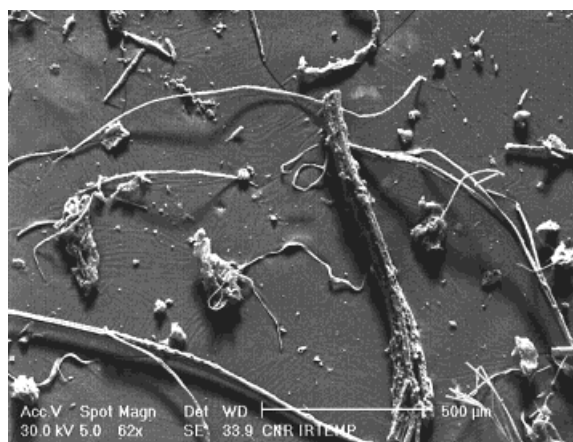
For both iPPMA-based composites series one can observe a slight increase in $T'_m[I]$ and X_c in the first fusion run for the composites with respect to the neat iPPMA. This fact probably can be attributed to the strong interactions between cellulosic fibers and iPPMA matrix. The fibers may “extract” selectively, the maleic anhydride groups (constitutional defects), from the polypropylenic backbone, leading to composites having a matrix characterized, on average, by a higher degree of constitutional regularity, with respect to the bulk in the neat iPPMA, and consequently higher T'_m and X_c .

Moreover, the increase of crystallization temperature in composites with respect to the neat

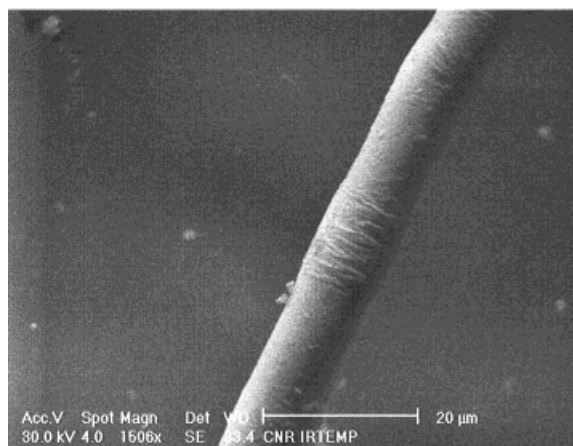
matrix can be attributed to the nucleating ability of the cellulosic fiber on the polymeric material as was observed by means of optical microscopy. For this purpose, in Figure 4(a,b), optical micrographs of iPPMA spherulites growing on a NaOH-extracted fiber are reported. These figures show a pronounced nucleating effect of the cellulosic fiber on the polypropylenic matrix. It is possible to note that the radius of the bulk crystallized spherulites and of the fiber nucleated spherulites seem to be comparable in their dimensions, so that only the nucleation and not the growth process is influenced by the presence of cellulosic fiber.

Tensile Tests

The values of tensile properties such as strength at break (σ_b), tensile modulus (E), and percent



(a)



(b)

Figure 3 SEM micrographs: SEP-extracted broom fibers. (a) $\times 40.3$; (b) $\times 686.4$.

Table II Summary of the Prepared Composites and Their Compositions

Materials	Composition (wt %)	Code
iPP	100/0	iPP neat
iPPMA	100/0	iPPMA neat
iPP/NaOH extracted fiber	50/50	iPP/broom 50/50
iPP/exploded fiber	50/50	iPP/broom SEP 50/50
iPPMA/NaOH extracted fiber	90/10	iPPMA/broom 90/10
iPPMA/NaOH extracted fiber	70/30	iPPMA/broom 70/30
iPPMA/NaOH extracted fiber	50/50	iPPMA/broom 50/50
iPPMA/exploded fiber	90/10	iPPMA/broom SEP 90/10
iPPMA/exploded fiber	70/30	iPPMA/broom SEP 70/30
iPPMA/exploded fiber	50/50	iPPMA/broom SEP 50/50
iPPMA/iPP/NaOH extracted fiber	5/45/50	iPPMA/iPP/broom 5/45/50
iPPMA/iPP/exploded fiber	5/45/50	iPPMA/iPP/broom SEP 5/45/50

elongation at break (ε_b) of the composites are shown in Table VI. From these parameters, the following considerations can be deduced: (1) iPP-based composites show a tensile Young's modulus comparable to that of iPP homopolymer. Conversely, the tensile strength at break and the percentual elongation at break show a sharp decrease compared to the neat matrix. These findings are probably due to weak fiber/matrix interfacial adhesion. (2) PPMA-based composites, reinforced with NaOH-extracted fibers, exhibit a strong increase of both Young's elastic modulus and tensile strength at break. These performances can probably be ascribed to a stronger fiber/matrix interface, caused by the interactions between maleic anhydride grafted on polypropylene and $-\text{OH}$ groups on cellulosic fibers. (3) The iPPMA-based materials reinforced with SEP-extracted fibers show only a slight decrease in tensile strength at break, while elastic modulus remains almost constant with respect to the neat iPPMA matrix.

(4) The two ternary composites, having a composition of 45% wt of iPP, 5% wt of iPPMA, and 50% wt of fibers, both NaOH treated and SEP extracted, present interesting behavior: their tensile properties are comparable with that of the related iPPMA-based material and also are higher with respect of iPP-based composites.

To explore the possibility for a more diffuse utilization of broom fiber composites in substitution for short glass fiber materials, a comparative analysis of properties of these two kinds of composites was performed, and the results are reported in Figure 5(a,b).¹⁵ In these graphics Young's modulus and tensile strength at break, normalized with respect of the materials density, are reported as a function of fiber content.

The trends of specific Young's modulus for the two types of composites show that the two materials have comparable behavior and, in particular, that the 50/50 broom fiber composite has a tensile modulus higher than the 70/30 glass fiber one.

Table III Apparent Melting Point Measured in the First and Second Fusion Run ($T'_m[\text{I}]$ and $T'_m[\text{II}]$), Crystallinity Content (X_c), Crystallization Temperature (T_c), and Glass Transition Temperature (T_g) of iPPMA-Based Composites Reinforced with NaOH Extracted Broom Fibers

Parameters	iPPMA Neat	iPPMA/Broom 90/10	iPPMA/Broom 70/30	iPPMA/Broom 50/50
$T'_m[\text{I}]$ ($^{\circ}\text{C}$)	160.0	160.9	160.8	161.6
X_c (%)	36.3	37.9	39.7	49.7
T_c ($^{\circ}\text{C}$)	115.2	117.8	120.7	123.7
X_c (%)	40.0	40.1	40.4	40.7
$T'_m[\text{II}]$ ($^{\circ}\text{C}$)	159.1	159.0	159.1	158.3
X_c (%)	36.7	38.6	38.3	35.9
T_g ($^{\circ}\text{C}$)	-10.8	-8.3	-5.2	-8.7

Table IV Apparent Melting Point Measured in the First and Second Fusion Run (T'_m [I] and T'_m [II]), Crystallinity Content (X_c), Crystallization Temperature (T_c), and Glass Transition Temperature (T_g) of iPPMA-Based Composites Reinforced with Exploded Broom Fibers

Parameters	iPPMA Neat	iPPMA/Broom SEP 90/10	iPPMA/Broom SEP 70/30	iPPMA/Broom SEP 50/50
T'_m [I] (°C)	160.0	160.9	161.7	162.2
X_x (%)	36.3	36.5	40.3	46.7
T_c (°C)	115.2	115.3	119.4	120.3
X_c (%)	40.0	46.8	39.8	44.3
T'_m [II] (°C)	159.1	159.7	157.4	156.0
X_c (%)	36.7	41.0	41.6	41.0
T_g (°C)	-10.8	-9.5	-8.8	-7.3

Furthermore, the broom fiber composites show, for all the examined compositions, an even higher specific tensile strength at break compared to the glass fibers reinforced materials. Therefore, the broom fibers show a reinforcement capability comparable to that of glass fibers.

Fracture Tests and Fractographic Analysis

The values of the critical strain energy release (G_c), and the critical stress intensity factor (K_c) for all the examined samples, calculated according to the LEFM theory, are reported in Table VII. The following conclusions are evident: (1) for iPP based composites G_c and K_c parameters remain almost constant for both types of fibers used as reinforcement; (2) on the contrary, for iPPMA-based composites, the two fracture parameters seem to increase linearly with fiber content, while a less pronounced improvement for the SEP fiber reinforced material is observed; (3) the two ternary composites present impact properties supe-

rior to those of iPP-based materials and similar to those of iPPMA-based composites, in agreement with the results of tensile tests.

The better performance found for the iPPMA-based composites should be ascribed to a stronger interfacial adhesion, produced by the presence of maleic anhydride.

The results of the fracture behavior can be interpreted on the basis of the fractographic analysis performed by SEM on the surface of the notched specimens. In Figures 6–9 the SEM micrographs of various composites, all taken near the notch tip in the region of crack initiation, are shown.

In Figure 6(a,b), the fracture surfaces of neat iPP and iPPMA are reported respectively, showing, in both cases, brittle behavior. No evidence of shear bands is observed. The finer texture found in the case of iPPMA sample reveals a nucleating effect owing, probably, to presence of the maleic anhydride.

Figures 7(a,b), and 8(a,b) show the SEM mi-

Table V Apparent Melting Point Measured in the First and Second Fusion Run (T'_m [I] and T'_m [II]), Crystallinity Content (X_c), Crystallization Temperature (T_c), and Glass Transition Temperature (T_g) of iPPA-Based Materials Reinforced Both with NaOH Extracted Fibers, Exploded Fibers, and of Ternary Composites

Parameters	iPPMA Neat	iPPMA/Broom 50/50	iPPMA/Broom SEP 50/50	iPPMA/iPP/Broom 5/45/50	iPPMA/iPP/Broom SEP 5/45/50
T'_m [I] (°C)	167.8	167.6	164.0	163.2	163.2
X_x (%)	40.4	50.2	45.7	51.5	51.0
T_c (°C)	117.3	124.3	122.3	125.2	121.5
X_c (%)	43.7	48.3	45.2	49.2	42.5
T'_m [II] (°C)	164.2	166.3	165.5	162.3	160.0
X_c (%)	38.0	42.7	40.3	49.7	42.5
T_g (°C)	-9.2	-8.8	-7.6	-14.7	-10.0

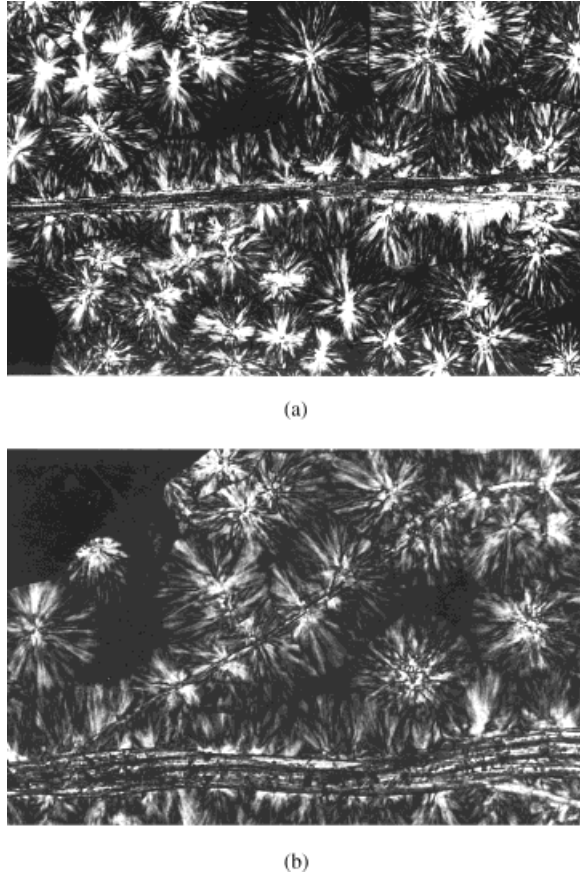


Figure 4 Optical micrograph: iPPMA spherulites growing on a NaOH-extracted fiber: (a) $T_c = 135^\circ\text{C}$, $\times 4.72$. (b) $T_c = 129^\circ\text{C}$, $\times 4.72$.

crographs relative to the fracture surfaces of the composites reinforced with 50% of broom fibers having as matrices iPP and iPPMA, respectively. From these figures the following can be noted: (1)

In the case of iPP-based composites, poor fiber/matrix interfacial adhesion is found for both NaOH-extracted fibers [Fig. 7(a)] and SEP extracted fibers [Fig. 7(b)]; this finding can be related to the difficulty of creating interactions between the cellulosic fiber and a non polar matrix. (2) The iPPMA-based composites show good interfacial adhesion between the two phases for both types of treated fibers. In particular, the SEM micrograph relative to the iPPMA/broom SEP [Fig. 8(b)] seems to present a higher degree of interaction between matrix and fiber with respect of that found in the case of iPPMA/broom NaOH extracted [Fig. 8(a)]. There is no evidence of pulled-out fibers, which appear to be well embedded inside the plastic matrix; however, a different feature is observed for the iPPMA/broom that has been NaOH extracted, where some pulled-out phenomena from the surface of material during the fracture are detected. (3) Concerning the two ternary blends, about the same behavior of binary iPPMA/broom fiber composites is found: the iPPMA/iPP/SEP-extracted broom fibers sample (in weight composition 5/45/50) [Fig. 9(b)] shows a very good fiber/matrix interconnection without the appearance of fibers pulled out from the polypropylenic matrices; in the case of the iPPMA/iPP/NaOH-extracted broom fibers composites (with a composition 5/45/50 wt) [Fig. 9(a)], although presenting a good fiber/matrix interfacial adhesion, some fibers are pulled out from the matrices.

Water Absorption Tests

One of the most undesirable properties of vegetable fibers is their dimensional instability due to

Table VI Young's Elastic Modulus (E), Tensile Strength at Break (σ_b) and Percent Elongation at Break (ϵ_b) of All the Samples

Materials	E (GPa)	σ_b (MPa)	ϵ_b (%)
iPPMA neat	1.2	18.3	2.0
iPPMA/broom 90/10	1.4	22.9	2.1
iPPMA/broom 70/30	1.8	27.6	2.2
iPPMA/broom 50/50	2.5	29.2	1.5
iPPMA/broom SEP 90/10	1.2	15.0	1.6
iPPMA/broom SEP 70/30	1.4	15.1	1.3
iPPMA/broom SEP 50/50	1.5	11.2	0.8
iPP neat	1.0	16.5	5.8
iPP/broom 50/50	0.8	9.5	1.6
iPP/broom SEP 50/50	1.3	3.2	2.2
iPPMA/iPP/broom 5/45/50	2.1	16.7	0.9
iPPMA/iPP/broom SEP 5/45/50	1.2	9.5	2.2

moisture absorption. This phenomenon is mainly caused by the hydrogen bonding between water molecules and the hydroxyl groups present in the cellulose structure. Clearly, a strong fiber/matrix interfacial adhesion can help to avoid the water penetration reducing the hygroscopicity, and, consequently, the worsening in the mechanical performances of materials.

Water absorption tests on our samples were performed according to the methods described in the Experimental section.

The results, shown as percent weight increase as a function of immersion time, are summarized in Figure 10, from which the following can be deduced: (1) as expected, the homopolymers (iPP and iPPMA) show the lowest water absorption;

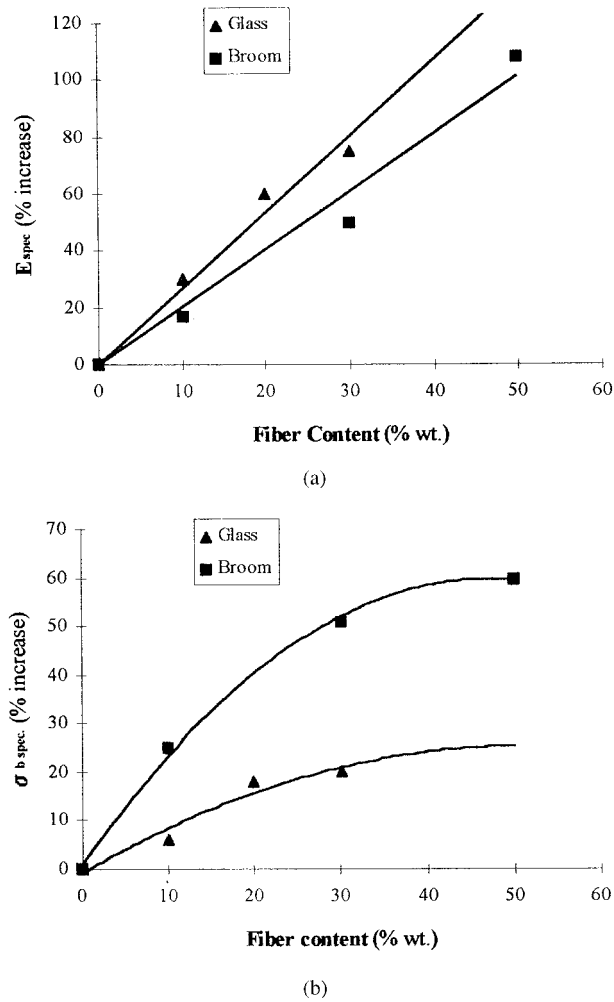


Figure 5 Tensile tests: percent increase in Young's elastic modulus (a) and in tensile strength at break (b) as a function of fiber content for glass-reinforced and NaOH-extracted broom fiber-reinforced composites both based on a polypropylenic matrix.

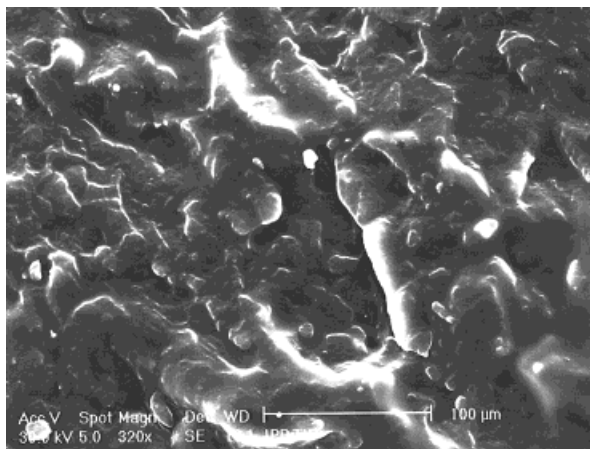
Table VII Critical Strain Energy Release (G_c) and Critical Stress Intensity Factor (K_{Ic}) for All the Samples

Materials	K_{Ic} (MN/m ^{3/2})	G_c (kJ/m ²)
iPPMA neat	0.82	0.77
iPPMA/broom 90/10	0.88	0.84
iPPMA/broom 70/30	1.64	1.91
iPPMA/broom 50/50	1.79	1.97
iPPMA/broom SEP 90/10	0.92	0.98
iPPMA/broom SEP 70/30	1.11	1.03
iPPMA/broom SEP 50/50	1.22	1.21
iPP neat	0.85	0.60
iPP/broom 50/50	0.95	0.52
iPP/broom SEP 50/50	0.93	0.50
iPPMA/iPP/broom 5/45/50	1.34	0.95
iPPMA/iPP/broom SEP 5/45/50	1.14	0.89

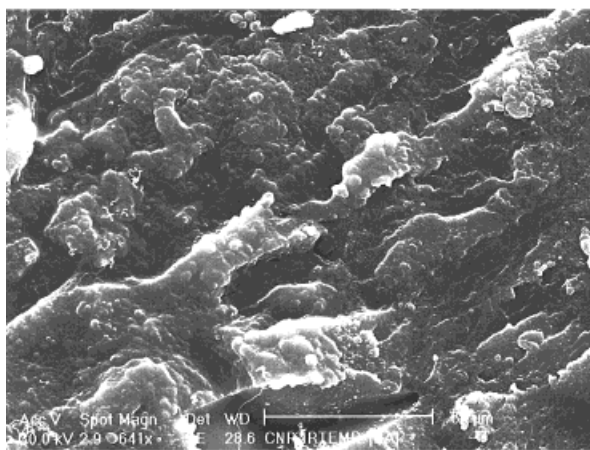
(2) the two iPP-based materials (iPP/broom 50/50 and iPP/broom SEP 50/50) are characterized by the shortest saturation time: the maximum water absorption was obtained after an immersion time of about 200 h; moreover, for these samples, the highest saturation percentage ($\sim 12\%$ wt) was found; clearly, these findings can be ascribed to the poor fiber/matrix adhesion as already shown by their mechanical behavior; (3) the two iPPMA-based composites reinforced with NaOH-extracted and SEP-treated fibers show different amounts of water absorbed. In the case of SEP-extracted fiber composites, a lower quantity of water penetrates than with the NaOH-extracted fiber materials. This finding is probably due to the lower crystallinity index of these latter fibers with respect to the exploded ones, as demonstrated by WAXS measurements. Moreover, the good fiber/matrix interfacial adhesion, obtained by using SEP-extracted fibers as reinforcements for iPPMA matrix, can also contribute to reduce the water absorption, as reported elsewhere;⁷ (d) the two ternary composites reveal, probably, also a strong fiber/matrix interface and have a low percentage of water absorbed at saturation and a long saturation time (for NaOH-extracted fiber composites about 7% of water absorbed and a saturation time of 800 h, for SEP fiber materials 9% and 800 h, respectively); this is in agreement with results of tensile and fracture tests.

Tensile tests, both on wet samples and dried (50°C for 24 h in an oven) were performed. The results of these tests are reported in Table VIII.

They confirm that a strong interface between



(a)



(b)

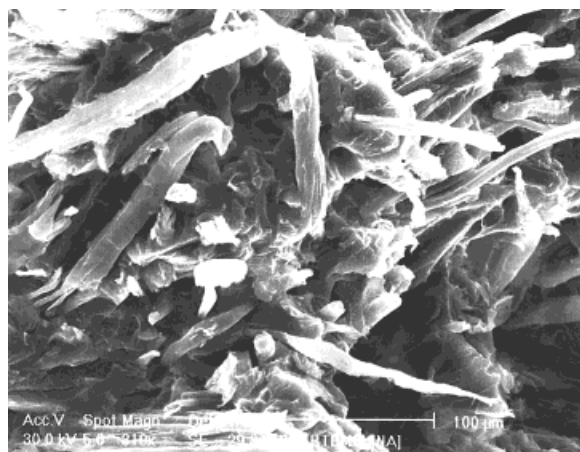
Figure 6 SEM micrographs: (a) fracture surface of iPP neat ($\times 208$). (b) fracture surface of iPPMA neat ($\times 416.65$).

cellulosic fiber and polypropylenic matrix leads to a reduction of the penetration of water, allowing only a slight worsening of tensile performance. The materials that show low water absorption, such as composites reinforced with SEP fibers, present only a slight decrease in tensile performances, and a subsequent oven treatment seems to restore the initial properties, indicating only a superficial water absorption. On the other hand, materials that are characterized by a large amount of absorbed water, such as iPP-based composites, show also a large reduction in mechanical properties; these features are not restored after an oven treatment, indicating deep penetration of water in the composite structure through the cellulosic fiber.

Finally, to determine the amount of water en-

trapped inside the materials, TGA was used to measure the weight reduction due to the evaporation of absorbed water in wet and dried samples both kept for 30 min at 140°C . In Table IX the results of these tests are summarized.

In the first column of the table the weight decreases, calculated for wet samples, are reported: all the water absorbed during immersion is released by the treatment; the values reported are in agreement with water saturation percentages shown in Figure 10. In the second column, the percents of water released by oven-treated samples are listed. In this way it was possible to determine the water absorbed in the inner structure of samples that cannot easily be released by oven heating. From these data it can be pointed out that the materials with low interfacial adhesion



(a)



(b)

Figure 7 SEM micrographs: (a) fracture surface of iPP/broom 50/50 ($\times 207.35$). (b) fracture surface of iPP/broom SEP 50/50 ($\times 196.3$).

(iPP/broom 50/50 and iPP/broom SEP 50/50) still show a large amount of diffused water in their structure (about 10% for both); on the contrary, for iPPMA-based materials the percent of retained water is lower. In particular, the SEP broom fiber-reinforced materials seem to present the best performances even in the case of ternary blends (about 0.5–1.0%), while a higher amount of water is found for the samples reinforced with NaOH extracted broom fibers (4.0% for the iPPMA/broom 50/50, and 1.7% for iPPMA/iPP/broom 5/45/50). These findings can explain the very good performances of SEP fiber-reinforced composites after immersion in aqueous medium, due to a slight superficial absorption of water that allows one to preserve the mechanical features of the materials.

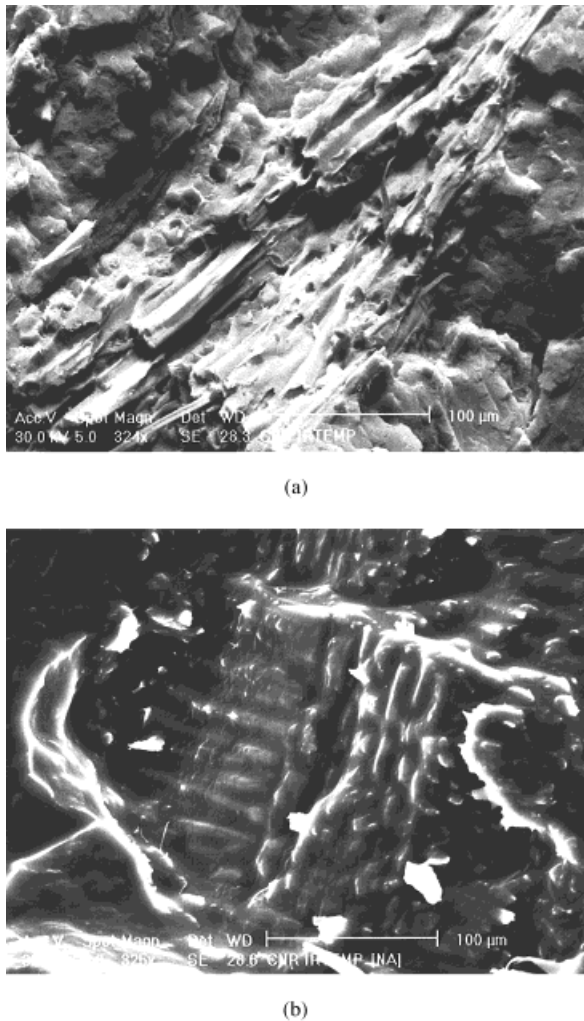
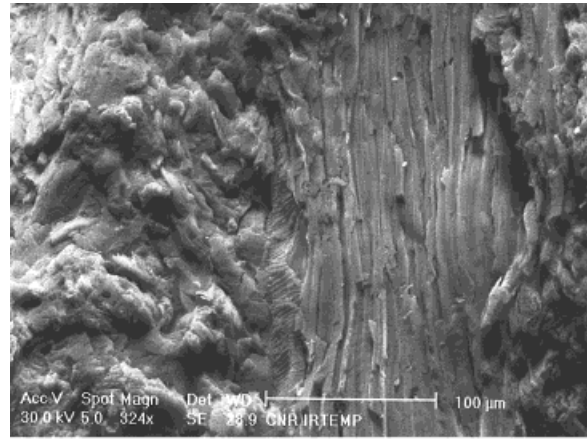
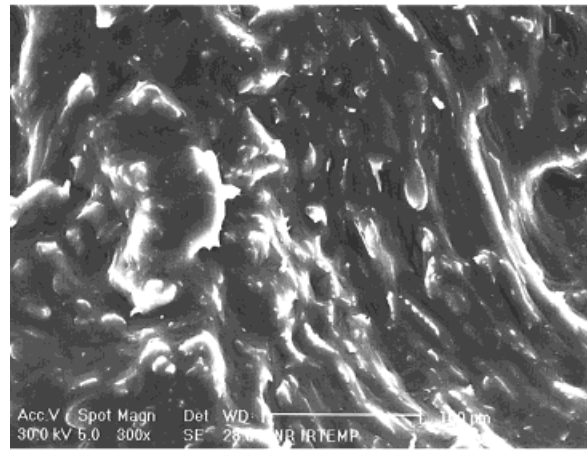


Figure 8 SEM micrographs: (a) fracture surface of iPPMA/broom 50/50 ($\times 210.6$). (b) fracture surface of iPPMA/broom SEP 50/50 ($\times 211.25$).



(a)



(b)

Figure 9 SEM micrographs: (a) fracture surface of iPPMA/iPP/broom 5/45/50 ($\times 210.6$). (b) fracture surface of iPPMA/iPP/broom SEP 5/45/50 ($\times 195$).

CONCLUSIONS

In this article the performances of iPP and iPPMA reinforced with broom fibers, extracted by using both a conventional alkaline treatment and an innovative steam explosion process, are studied.

The following conclusions from the results can be drawn:

1. Broom fibers obtained by steam explosion seem to produce better fiber/matrix interfacial adhesion with respect to those extracted by alkaline treatment, as clearly shown by SEM analysis and water absorption tests. Nevertheless, the mechanical behavior of composites reinforced with NaOH-extracted broom fibers is superior with respect to that

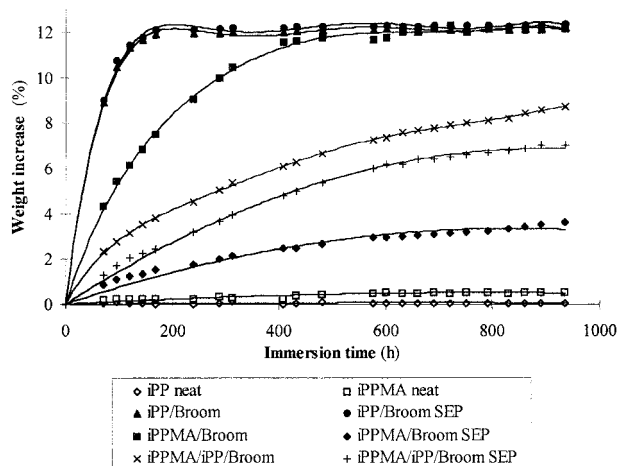


Figure 10 Water absorption tests: weight increase of the samples as a function of time.

of the SEP fiber composites; this finding can probably be attributed to the minor structure damage produced by the chemical treatment that allows one to obtain longer and bundled fibers.

2. The utilization of an iPPMA matrix as an alternative to a conventional polypropylene, as previously shown,⁷ produces composites with good final properties. This occurs because of the presence of maleic groups that are able to create a strong interface between matrix and cellulosic material.
3. The strong affinity of the iPPMA matrix for the lignocellulosic fibers was also demonstrated by the behavior of the two ternary blends. These were prepared by using a matrix constituted of 90% of iPP and only 10% of iPPMA, and they present properties very similar to those of whole iPPMA-based composites. A possible explanation of this finding can be given by supposing that the cellulosic fibers “capture” the maleated polypropylenic chains by creating an esteric linkage between the cellulosic —OH and the maleic anhydride molecules grafted on the polypropylenic backbone,⁷ at the same time excluding the iPP-bulk to participate at the interface.
4. The use of SEP fibers as reinforcement for iPPMA-based composites contribute to reduce

Table VIII Young’s Elastic Modulus (E), Tensile Strength at Break (σ_b) and Percent Elongation at Break (ε_b) Performed Before (Anhydrous) and After (Wet) Water Absorption, and Also After 24 h in Oven at 50°C (Dried)

Materials	E (GPa)	σ_b (MPa)	ε_b (%)
iPPMA neat (anhydrous)	1.2	18.3	2.0
iPPMA neat (wet)	1.1	16.0	1.9
iPPMA neat (dried)	1.2	17.3	1.9
iPPMA/broom 50/50 (a)	2.5	29.2	1.5
iPPMA/broom 50/50 (w)	1.4	14.6	3.2
iPPMA/broom 50/50 (d)	2.0	22.7	2.7
iPPMA/broom SEP 50/50 (a)	1.5	11.2	0.8
iPPMA/broom SEP 50/50 (w)	1.5	11.0	1.2
iPPMA/broom SEP 50/50 (d)	1.5	11.2	0.9
iPP neat (a)	1.0	16.5	5.8
iPP neat (w)	0.8	15.4	5.5
iPP neat (d)	0.8	16.4	5.4
iPP/broom 50/50 (a)	0.8	9.5	1.6
iPP/broom 50/50 (w)	0.5	6.9	2.3
iPP/broom 50/50 (d)	0.5	6.5	1.6
iPP/broom SEP 50/50 (a)	1.3	3.2	2.2
iPP/broom SEP 50/50 (w)	0.8	2.3	3.2
iPP/broom SEP 50/50 (d)	0.8	2.2	2.2
iPPMA/iPP/broom 5/45/50 (a)	2.1	16.7	0.9
iPPMA/iPP/broom 5/45/50 (w)	1.8	13.6	1.0
iPPMA/iPP/broom 5/45/50 (d)	1.7	14.9	0.9
iPPMA/iPP/broom SEP 5/45/50 (a)	1.2	9.5	2.2
iPPMA/iPP/broom SEP 5/45/50 (w)	1.0	7.7	2.4
iPPMA/iPP/broom SEP 5/45/50 (d)	0.9	8.7	2.2

Table IX Weight Percent of Released Water in Wet Samples and in Dried Ones After Treatment in an Oven for 24 h at 50°C, Determined by Means of Thermogravimetry

Materials	Weight Percent of Released Water	
	Wet Sample	Dried Sample
iPPMA neat	Not evaluated	Not evaluated
iPPMA/broom 50/50	11.5%	4.0%
iPPMA/broom SEP 50/50	3.5%	0.5%
iPP neat	Not evaluated	Not evaluated
iPP/broom 50/50	11.9%	10.0%
iPP/broom SEP 50/50	12.1%	10.3%
iPPMA/iPP/broom 5/45/50	8.5%	1.7%
iPPMA/iPP/broom SEP 5/45/50	6.7%	0.9%

the penetration of water in the structure with respect to the NaOH-extracted fibers: this effect can be due both to the higher crystallinity of the SEP fibers that reduces the water diffusion through the amorphous region, and to better fiber/matrix interfacial adhesion.

5. The NaOH-extracted fiber iPPMA-based composites present specific mechanical properties comparable to those of analogous short glass fiber reinforced materials; this can lead, in the future, to a real possibility for broom fibers to be used as alternative materials to the standard synthetic reinforcement, also owing to the fact that they are cheap, light, and biodegradable.

The authors thanks Prof. R. Palumbo of the University "Federico II" of Naples for some helpful discussions, Mr. G. Della Volpe, Mr. G. Orsello, and Mr. V. Di Liello of the IRTeMP-CNR for their help in performing optical microscope analysis, SEM analysis, and mechanical tests, respectively.

REFERENCES

1. P. Zadorecki and A. J. Michell, *Polym. Compos.*, **29**, 69 (1989).
2. J. F. Kennedy, G. O. Phillips, and P. A. Williams, *Wood Processing and Utilizations*, Ellis Horwood, UK, 1989.
3. D. Maldas and B. V. Kokta, *Int. J. Polym. Mater.*, **14**, 165 (1990).
4. M. Dalvåg, C. Klason, and H. E. Strömvall, *Int. J. Polym. Mater.*, **11**, 9 (1985).
5. C. Klason, J. Kubát, and H. E. Strömvall, *Int. J. Polym. Mater.*, **10**, 159 (1984).
6. M. Avella, E. Martuscelli, B. Pascucci, M. Raimo, B. Focher, and A. Marzetti, *J. Appl. Polym. Sci.*, **49**, 2091 (1983).
7. M. Avella, C. Bozzi, R. dell'Erba, B. Focher, A. Marzetti, and E. Martuscelli, *Angew. Makromol. Chem.*, **233**, 149 (1995).
8. B. Focher, A. Marzetti, and V. Crescenzi, *Steam Explosion Techniques: Fundamentals and Application*, Gordon and Breach Science Publishers, Philadelphia, PA, 1991, p. 331.
9. R. M. Marchessault, S. Coulomba, H. Morikawa, and D. Robert, *Can. J. Chem.*, **60**, 2372 (1982).
10. S. N. Maiti and R. Subbarao, *Int. J. Polym. Mater.*, **15**, 1 (1991).
11. R. P. Quirk and M. A. A. Alsamarraie, *Polym. Handbook*, 3rd ed., V-31, John Wiley & Sons, New York, 1989.
12. A. J. Kinloch and R. J. Young, *Fracture Behaviour of Polymers*, Applied Science Publishers, London, 1983.
13. F. Coppola, R. Greco, and G. Ragosta, *J. Mater. Sci.*, **21**, 1775 (1986).
14. L. Segal, J. J. Creely, A. E. Martin, Jr., and C. M. Conrad, *Text. Res. J.*, **29**, 786 (1959).
15. From *FRP Design Data Book*, published by Fiberglass Limited, UK, 1969.